Supplement of Atmos. Chem. Phys., 21, 2931–2943, 2021
https://doi.org/10.5194/acp-21-2931-2021-supplement

Atmospheric Chemistry and Physics
Open Access
EGU

Supplement of

Deposition of light-absorbing particles in glacier snow of the Sunderdhunga Valley, the southern forefront of the central Himalayas

Jonas Svensson et al.

Correspondence to: Jonas Svensson (jonas.svensson@fmi.fi)

Supplement

1. Snow pit profiles

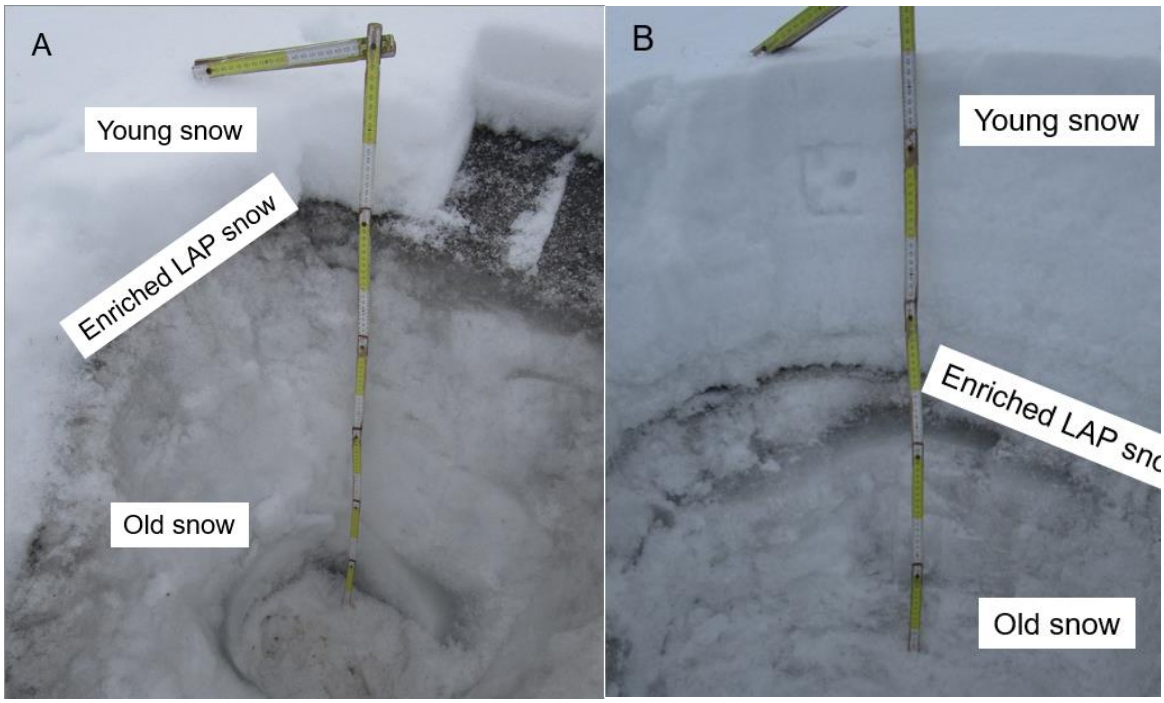

Figure S1. In A) Snow pit B from 2016 with while in B) pit D is shown.

2. Snow depth and albedo with AWS

Albedo data processing: first, the SW radiation baselines values were adjusted to, +10 and +2.5 W m^{-2} for incoming and outgoing radiation, respectively. Second, incoming SW radiation had to be equal or greater than outgoing SW radiation. This filter mainly removes noisy data during the dark period of the day, but also episodes when the sensors are potentially covered by snow. Third, an albedo value of 0.2 was used to distinguish bare conditions from periods where there is sufficient amount of snow on the ground.

Snow depth data processing: the last adjustment to the AWS data is related to the maximum snow depth (SD) that is nominally achievable. The sensor is determined to be at a level of 192 cm above the ground surface. The sensor should have at least a distance of 0.5 m between the sensor and the snow surface. Hence, practically the maximum SD is 142 cm. However, we have used data up to 156 cm. At this SD we note a clear change in response and the sensor have obvious difficulties to determine SD. On a few instances, the SD depth is negative while there is obviously a thick snow cover. We suspect that this is due to snow depth greater than 156 cm and that the sending and receiving of pulses is not synchronized and interpreted as negative snow depths. For these limited periods, we have added the absolute value of the negative snow depth to 156 cm if at the same time the snow albedo is at least 0.6 and the new SD

does not exceed 190 cm. This last adjustment improves the consistency between snow albedo and SD but does little to the accumulated snow estimates.

Averaging: finally, we applied a moving 24 hour median filter to all the AWS data.

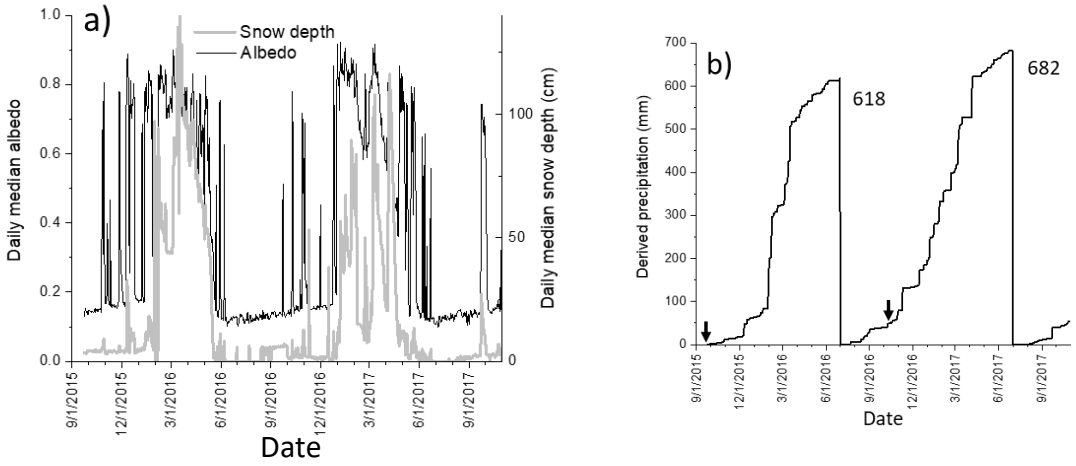

Figure S2. In a) the daily median snow depth is plotted together with the daily median albedo. In b) the integrated positive changes in the snow depth is converted to precipitation assuming a snow density of 0.1 g m^{-3}. On 1 July, the integration is reset to zero. The integrated precipitation amounts for the two annual cycles are indicated in the figure. The time of sampling in 2015 and 2016 are indicated by the small arrows.

3. Determining TC/EC ratio for unsaturated filter samples

When plotting filter samples where the EC amounts were assumed to be reliable (i.e. excluding the 17 samples where accurate EC determinations could not be done), it became evident that some data points were unsatisfactory—containing elevated LAP loadings, lowering the EC:TC ratio (Fig. S3a). Therefore, the data was excluded according to: TC lower than 100 µg cm^{-2}, as well as an optical depth of less than two. With these data points removed (N=11), the EC:TC resulted in a higher slope (Fig. S3a+b). Since the offset will be negligible for the samples where EC is reconstructed, it was here ignored. The 17 samples where accurate EC determinations could not be done were reconstructed with the slope of 0.099.

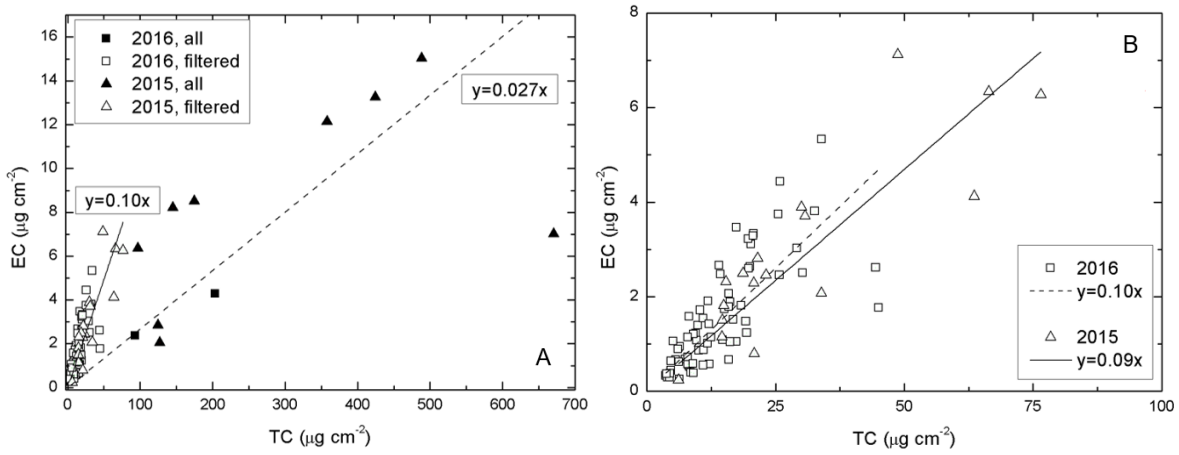

Figure S3. EC TC ratio for (a) All filter samples, as well as excluded data points; and (b) only excluded data points.

4. Determining suitable common effective constants for young and old snow (EC_y^* and EC_o^*), respectively.

In order to define the constants EC_y^* and EC_o^* we systematically changed the constants over a range of values and plotted (in Fig. S4) the returned slope from the linear fit between observed ECacc and calculated ECacc. Where the linear fit returns a slope of 1, the ideal EC*constant is found. Evident in Fig. S4, the precise EC_y^* constant is slightly more than 50 µg L^{-1}, while the EC_o^* constant is somewhat lower than 150 µg L^{-1}. For convenience and simplicity, however, we chose to work with the numbers 50 and 150 for EC_y^* and EC_o^*, respectively.

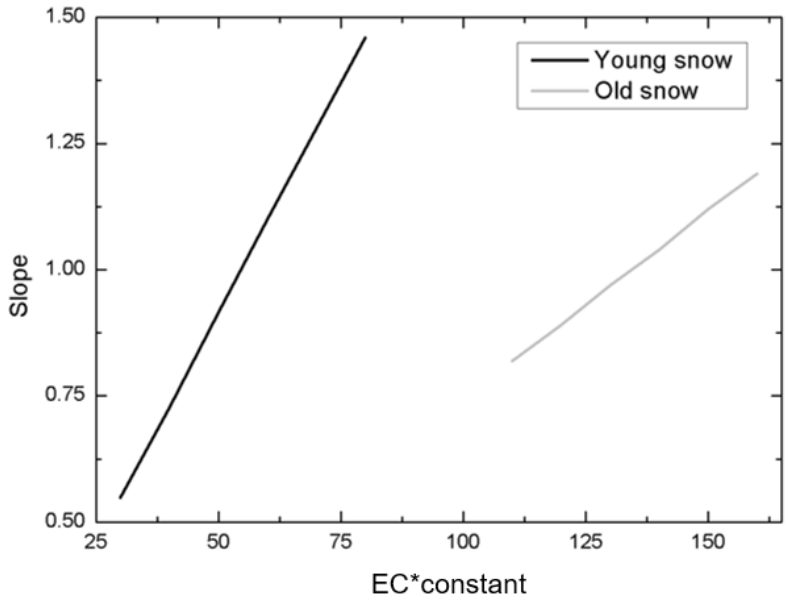

Figure S4. Different constants EC_y^* and EC_o^* and their corresponding slopes returned from linear fits between observed and calculated ECacc.